233 (2024) 212541

Contents lists available at ScienceDirect

Geoenergy Science and Engineering

journal homepage: www.sciencedirect.com/journal/geoenergy-science-and-engineering

Study of calcium carbonate scaling on steel using a high salinity brine simulating a pre-salt produced water

Juliana Francisco de Angelo, Jean Vicente Ferrari *

Universidade de São Paulo, Escola Politécnica, Departamento de Engenharia de Minas e de Petróleo, Av. Prof Mello de Moraes 2373, São Paulo, SP, CEP, 05508-030, Brazil

ARTICLE INFO

Keywords:
Pre-salt
Calcium carbonate scale
Surface effects
Carbon steel
Corrosion

ABSTRACT

In Brazilian pre-salt production, high carbon dioxide (CO_2) levels in the associated gas, high salinity in the water, and high levels of calcium ions cause problems related to corrosion and scale. In practice, the scaling process already begins in the formation and near the wellbore region. However, this work has addressed this issue only on a steel surface, representing what can occur in oil production tubings and equipment since the build-up of these products in the internal walls can also impact the production flow guarantee. Parameters related to the substrate and the environment can influence calcium carbonate ($CaCO_3$) precipitation mechanisms. In this study, the effect of steel surface roughness on calcium carbonate scaling experiments has been studied in a high salinity brine containing sodium bicarbonate ($NaHCO_3$) and calcium chloride ($CaCl_2$), simulating pre-salt produced water and under flow conditions. The scaling tests were carried out with a set-up composed of a peristaltic pump to recirculate the test solution through a flow cell. The scale build-up was analysed by using techniques such as Inductively Coupled Plasma Optical Emission Spectrometry (ICP-OES), X-ray Diffraction (XRD), Scanning Electron Microscopy (SEM), and Energy Dispersion X-ray Spectroscopy (EDS). For tests carried out in 3 h, the smoother surfaces had lower adhesion of calcium carbonate than surfaces with higher roughness. Lepidocrocite and rokuehnite, which are corrosion products, were formed in the substrates with higher roughness values, promoting aragonite formation. This work demonstrates that roughness influences calcium carbonate scale formation under flow conditions, besides affecting the calcium carbonate polymorphs associated with the corrosion process.

1. Introduction

The discovery of pre-salt carbonate reservoirs in Brazil is one of the most important in the oil and gas exploration area in recent years. The pre-salt reservoir contains large accumulations of excellent quality and light oil (28–30° API), which places Brazil in a strategic position given the great demand for energy worldwide (Beltrao et al., 2009; Drexler et al., 2020).

In some areas of Brazilian pre-salt production, the CO_2 content in the associated gas can be above 20% (Cezar et al., 2015). This high salinity environment, which contains CO_2, in addition to high levels of calcium ions that can reach the order of 10,000 ppm (Bezerra et al., 2013), can cause problems related both to corrosion and calcium carbonate scaling. This can impact the production flow guarantee, mainly because fluids flow through long pipelines, and access to the pipes and equipment is difficult due to the depth of the wells (Santana and Manzela, 2016).

Inorganic scales are inorganic salt deposits found in reservoirs, pipes, and equipment used in oil production and are considered one of the significant problems in the oil industry. Scale build-up reduces the area available for the passage of fluids through the accumulation of mineral substances in the metal walls, resulting in a decrease in production and time squandered removing the material, causing production losses (Crabtree et al., 1999; Liu et al., 2022; Olajire, 2015; Vazirian et al., 2016).

To control scale formation, it is necessary to understand both the environment and the substrate. Knowing the formation conditions, it is possible to understand how to remove it and develop treatments to restore the productivity of the wells in the long term since the production shutdown and expenses incurred by scale removal are economically significant (Chaussemier et al., 2015; Crabtree et al., 1999).

Piping and equipment behave differently when exposed to scaling. The adhesion, morphology, and toughness of deposits formed on

* Corresponding author. Universidade de São Paulo, Escola Politécnica, Departamento de Engenharia de Minas e de Petróleo, São Paulo, SP, Brazil.
E-mail address: jeanferrari@usp.br (J.V. Ferrari).

https://doi.org/10.1016/j.geoen.2023.212541
Received 6 December 2022; Received in revised form 21 October 2023; Accepted 24 November 2023
Available online 30 November 2023

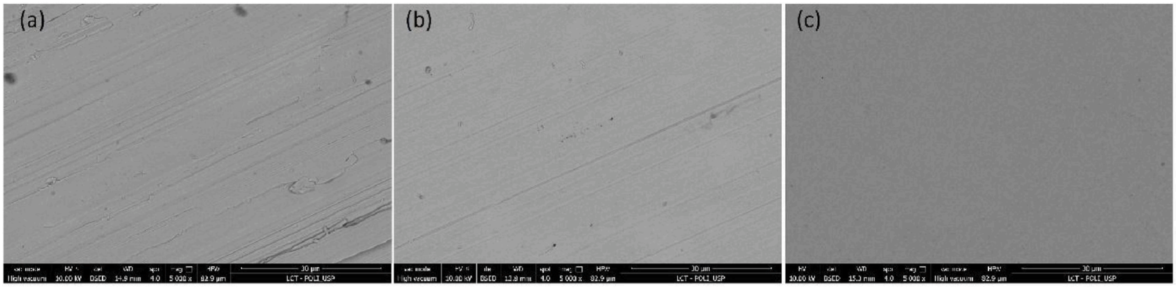

Fig. 1. SEM images of the substrates used in this work. (a) #120, (b) #1200 and (c) 1 μm.

surfaces depend on two types of parameters: physical-chemical properties (aqueous solution chemical composition, supersaturation level, temperature, and flow) and substrate properties (nucleation sites, surface free energy, surface roughness, wettability, among others) (Cheong et al., 2013; Eroini et al., 2011; Liu et al., 2011; Marques et al., 2001).

According to Cheong et al. (2013), when a substrate is present, the formation of crystals can occur by heterogeneous nucleation. The ion cluster accumulates on the surface, followed by the growth of the crystals. Crystals formed on the substrate by heterogeneous nucleation are more adherent, compact, and resistant than crystals formed in one part of the system and transported to another.

A lot of research has been focused on the study of the effects of the scale formed on different substrates materials and surface treatments (Chen et al., 2005; Droguett et al., 2015; Eroini et al., 2011; Liu et al., 2011; Neville and Morizot, 2000; Sanni et al., 2017; Vazirian et al., 2016; Wang et al., 2013; Yamanaka et al., 2009).

Hidema et al. (2016) mention that scaling is affected by substrate roughness and that smooth surfaces are more likely to prevent scaling. Zettler et al. (2005) analysed the scale formation on stainless steel surfaces subjected to various surface treatments. They concluded that in treatments that provided rougher surfaces, there was a greater tendency for scale formation. Wang et al. (2005) highlight surface energy and roughness in $CaCO_3$ formation, showing that roughness may be a more dominant factor in scaling formation on surfaces with similar surface energies due to increased hooking sites on the rougher substrates.

The substrate chosen for this work is a low-carbon steel, a less popular material in calcium carbonate scaling studies, although widely used in the oil and gas industry due to low costs and is used in a wide range of structures and equipment in this area (Palmer and King, 2004; Telles, 2001). Due to the low corrosion resistance of carbon steel, most calcium carbonate scaling studies choose stainless steels as a substrate (Chen et al., 2005; Liu et al., 2011; Vazirian et al., 2016), which is more expensive than carbon steel. Moreover, studies are comparing different types of anti-scaling coatings applied to these metallic substrates (Eroini et al., 2011; Vazirian et al., 2016), in addition to a few others analysing surface finishing by sanding to correlate the substrate's roughness with calcium carbonate scale adhesion (Liu et al., 2011).

It is important to mention that surface roughness also influences the corrosion of metallic substrates (Abosrra et al., 2009; Toloei et al., 2013) which may further prompt the adhesion of $CaCO_3$ fouling (Liu et al., 2011).

This work aims to study the formation of calcium carbonate scale using a brine containing a calcium content close to that found in the pre-salt produced water on a carbon steel surface with different roughness levels achieved mechanically, using sandpaper. Concerning the flow effect on scaling, literature reports several experimental set-ups using rotating cylinder electrodes (Cheong et al., 2013), rotating disk electrodes (Vazirian et al., 2016), and submerged impinging jets (Wang et al., 2005), among others, depending on the objective of the work. In this work, the scaling tests were carried out with a set-up composed of a peristaltic pump to recirculate the test solution through a flow cell.

2. Calcium carbonate scale formation in oil and gas production

The formation water, inside the reservoir, contains bicarbonate ions (HCO^{3-}) which are in equilibrium with the carbonate ions (CO_3^{2-}) represented by eq. (1) (Kelland, 2009):

$$2HCO_3^- \leftrightarrows CO_3^{2-} + H_2O + CO_2(g) \tag{1}$$

In oil production, according to Le Chatelier's principle, when the pressure decreases, CO_2 is released from the liquid phase, and the equilibrium of eq. (1) move to the right, in the direction of carbon dioxide (CO_2) production, to increase the pressure to reach equilibrium again. As a consequence, carbonate ions are formed, and pH is increased (Kelland, 2009).

Another source of carbonate and bicarbonate ions in the formation water is due to the presence of carbon dioxide dissolved in the water shown by eq. (2), eq. (3) and eq. (4). Carbon dioxide, when dissolved, forms carbonic acid (H_2CO_3) due to ionic dissociation. The carbonic acid produces bicarbonate ions and hydrogen ions (H^+). The bicarbonate ion also undergoes ionic dissociation into carbonate ions and hydrogen ions (Olajire, 2015; Qazvini et al., 2021).

$$CO_2 + H_2O \leftrightarrows H_2CO_3 \tag{2}$$

$$H_2CO_3 \leftrightarrows H^+ + HCO_3^- \tag{3}$$

$$HCO_3^- \leftrightarrows H^+ + CO_3^{2-} \tag{4}$$

Calcium ions (Ca^{2+}) are also present in the formation water and when in contact with carbonate ions, calcium carbonate is produced, represented by eq. (5). Calcium carbonate concentration increases until it reaches a point that is high enough to start the precipitation of this compound.

$$Ca^{2+} + CO_3^{2-} \rightarrow CaCO_3\downarrow \tag{5}$$

Calcium carbonate deposition is dependent on pH, temperature, the concentration of calcium ions and bicarbonate ions, and ionic strength. Precipitation increases with increasing temperature and pH and decreasing pressure (Kamal et al., 2018).

Calcium carbonate scale can be found in three crystalline polymorphisms: calcite, aragonite, and vaterite. Vaterite is the least stable among these three morphologies (Wang et al., 2005), while calcite is the most common form of scale (Maciel et al., 2017).

Wang et al. (2005) mention that the development of these three crystalline polymorphisms depends on the formation conditions. It is thought that these different morphologies will have varying properties regarding their adhesion to surfaces. Liu et al. (2011) relate that aragonite is prone to form when there is a corrosive process of a ferrous substrate. Additionally, Hashimoto et al. (2017) have shown that the average amount of calcium carbonate deposited on the surface of carbon steel (10.1 g/m^2) was slightly higher than on stainless steel (9.5 g/m^2) and that the weight ratio (w/w %) of calcite form adhered on stainless steel (74.5%) was higher than on steel (55.7%).

These researches show that these material's substrates influenced

Fig. 2. Gradual calcium carbonate formation in the solution at 25 °C.

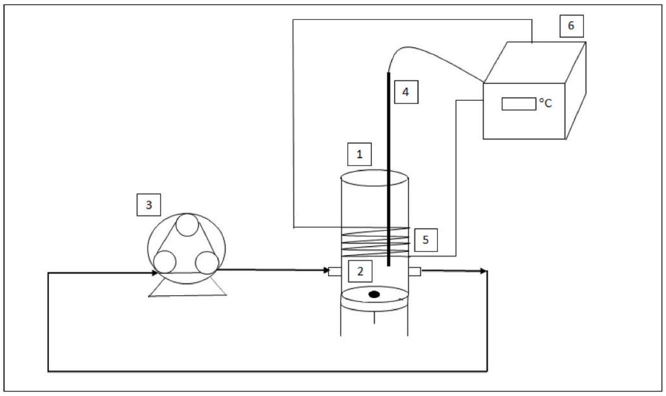

Fig. 3. The schematic diagram for the experimental equipment. 1. Flow cell, 2. Steel sample, 3. Peristaltic pump, 4. Thermocouple, 5. Flexible silicone electric resistor, 6. Temperature controller.

Table 1
Table of experiments – Grit sizes and experiment time.

Test Number	Grit sizes	Experiment time
01	120#	10 min
02	120#	30 min
03	120#	1 h
04	120#	3 h
05	1200#	10 min
06	1200#	30 min
07	1200#	1 h
08	1200#	3 h
09	Polished (1 μm)	10 min
10	Polished (1 μm)	30 min
11	Polished (1 μm)	1 h
12	Polished (1 μm)	3 h

calcium carbonate's growth and highlight the importance of considering both substrates used in the oil and gas industry in the scaling studies.

3. Experimental methodology

3.1. Substrate

To study the calcium carbonate scale on metal surfaces representing what can occur in oil production tubings and equipment, the substrate selected for this work was carbon steel (AISI 1010). The samples were disks of approximately 10 mm in diameter. Before the scaling experiments, the steel specimens were roughened using abrasive papers (grits sizes: #120, #1200 - ANSI/CAMI) and polished with 1 μm diamond paste (mirror-like finish). To analyze the sample surfaces before (without scale) and after (with scale) scaling tests, SEM (Scanning electron microscopy) images were used. Before scaling tests, SEM images of these surfaces, obtained using the back-scattered electron mode (accelerating voltages of 10 kV) are shown in Fig. 1. After this procedure, the specimens were cleaned with acetone and alcohol, followed by drying using compressed air.

3.2. Saline solution

This study's focus is a saturated brine to obtain a calcium carbonate scale on metallic surfaces of different roughness. The solution contained sodium bicarbonate ($NaHCO_3$) (3.36 g/L), sodium chloride (NaCl) (100 g/L), and calcium chloride ($CaCl_2.2H_2O$) (36.75 g/L). Each reagent was separately dissolved in distilled water, before these solutions were mixed. After that, the mixed solution was added to a flow cell before $CaCO_3$ precipitate formed. The solution was prepared at 25 °C. The pH solution was 6.1 after preparation, and the solution saturation index is 5.82, which indicates a supersaturated condition with respect to calcium carbonate precipitation.

In the flow cell, the solution was heated to 60 °C and then gradually became cloudy for a few seconds (around 20 s), allowing scaling tests to be performed without CO_2 bubbling, because the calcium carbonate precipitate starts to form when in contact with the steel, inside the flow cell. This methodology intends to represent what happens in oil production when the produced water comes into contact with the production tubings.

Fig. 2 shows the calcium carbonate formation from the beginning of the mixture to approximately 120 s.

Eq. (6) shows the chemical reaction that occurs in the test saline solution:

$$CaCl_2 + 2NaHCO_3 \rightarrow CO_2 + CaCO_3 + 2NaCl + H_2O \tag{6}$$

3.3. Scaling tests

Fig. 3 represents the equipment developed for this work. The equipment was composed of a peristaltic pump SEKO, PR-120 model, a 250 ml glass flow cell and a temperature controller connected to a flexible silicone electrical resistor and a thermocouple.

The equipment was constructed to recirculate the test solution through the flow cell (approximately flow rate: 90L/h), controlling the temperature with a controller coupled to a flexible silicone electrical resistor and a thermocouple. The steel sample, embedded in epoxy resin or Bakelite, was placed inside the cell in a horizontal position (as shown in Fig. 3) that was in contact with the flow recirculated by the pump.

This flow rate of 90 L/h represents approximately a flow velocity of 0.3 m/s, considering a 1 cm^2 silicon tubing internal diameter used on the flow cell, which represents a turbulent flow regime (Re~ 4,200, with a viscosity of the solution of 0.0008 Pa.s and solution density of 1.05 g/ cm^3 @ 60 °C). This flow feature is within the range of other published works concerning scale build-up on metal surfaces for the oil and gas production area or in scaling processes on heat transfer surfaces. Vazirian et al. (2016) used a rotating cylinder electrode constructed of stainless-steel substrate coated with various industrial coatings to study inorganic scale deposits, including the $CaCO_3$. In their experimental approach, samples were rotated in brine at two rotational speeds, which produced surface velocities of 0.01256 m/s (laminar) to 1.256 m/s (turbulent). An increase in the bulk's turbulence increased the surface's scale formation rate in deposition and adhesion processes. Moreover, Wang et al. (2016), in their experimental work, presented a literature review focused on studying the effects of $CaCO_3$ scaling on heat transfer surfaces and summarized that the flow velocity mainly studied ranged from 0.2 m/s to 1.6 m/s, and the turbulent flow was considered.

The solution was added to the equipment immediately after mixing $NaHCO_3$, NaCl and $CaCl_2.2H_2O$ solutions, at 25 °C, as mentioned in item 3.2. When the solution is added, it is still transparent and becomes cloudy only when it is circulating through the equipment. A 200 W electrical immersion resistance heater without a thermostat helped the initial temperature of the solution to reach 60 °C in approximately 5–8 min and from this moment this heater was removed from inside the cell and the controller maintained the temperature of 60 °C during all tests.

The experiments were conducted for 10 min, 30 min, 1 h and 3 h. At the end of this period, the sample was removed from the cell, washed

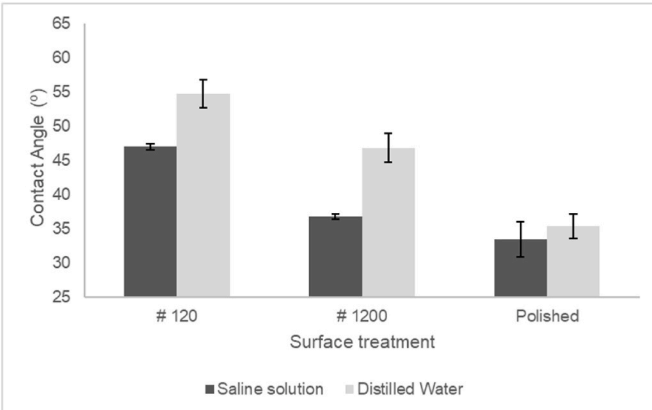

Fig. 4. Contact angle measurements results for samples roughened using abrasive papers (# 120, # 1200) and polished (with 1 μm diamond paste).

Table 2
Roughness results.

Sample	R_a (μm)	Error
#120	0.6821	0.0002
#1200	0.0210	0.0013
Polished (1 μm)	0.0015	0.0001

with distilled water and dried with compressed air. Table 1 shows the experiments carried out. Each test was carried out in triplicate. All tests were conducted with temperature of 60 °C and atmospheric pressure and test solution prepared with sodium bicarbonate ($NaHCO_3$) (3.36 g/L), sodium chloride (NaCl) (100 g/L), and calcium chloride ($CaCl_2.2H_2O$) (36.75 g/L) (item 3.2 – saline solution). In this proposed flow cell, although not approached in this work, it is supposed that lower flow velocities could increase the scale build-up due to the horizontal substrate exposition on this cell (Fig. 3). The pH of the final solution (after mixing the salts) was 6.1, allowing the $CaCO_3$ precipitation. Pomini (2013) indicated a range of simulated pH's from 5.2 to 5.8, considering the oil production from the Christmas tree and the primary processing equipment in a fluid containing 2.8% CO_2 in the gas phase.

3.4. Surface characterisation

3.4.1. Contact angle measurements

Contact angle analysis has been used in scaling studies to characterise the surface affinity with the test solution, evaluating the surface wettability, as the tendency to surface scale is dependent on the substrate surface energy (Eroini et al., 2011).

The contact angle measurements between each substrate and solution were taken using the sessile drop method. The equipment used for this analysis was the Drop Shape Analyzer (DSA-25), Kruss. The equipment has a syringe that deposits a drop of solution on the substrate surface and measure the contact angle between them. The needle used was 0.510 mm. The analysis was performed in open-air conditions at a room temperature of 20 °C. The substrates used were carbon steel samples roughened using abrasive papers (grits sizes: #120, #1200) and polished with 1 μm diamond paste, cleaned with acetone and alcohol and dried with compressed air. The analysis was performed with the previously described test solution and distilled water. The contact angle measurements were performed in triplicate and to standardise the reading of the samples, they were measured 2 min after the drop.

3.4.2. Surface roughness

Profilometry was used to evaluate the surface topography to identify the roughness influences on the calcium carbonate scale mechanism formation. The steel surface roughness (R_a, roughness average) was measured by a Taylor-Hobson 3D CCI Profilometer which uses interferometric measurement.

3.5. Scale analysis

3.5.1. X-ray diffractometer (XRD)

X-ray diffraction was used for the chemical analysis of the scaling deposited in the samples after carrying out the calcium carbonate scaling experiments. The diffractometer was a Panalytical X'Pert PRO, with a Cu target and X'Celerator position sensitive detector. The analytical conditions (CuKα radiation, 45 kV, 40 mA, step of 0.02°/s) were maintained constant in the interval of 2–70°, 2θ, for all samples.

3.5.2. Inductively Coupled Plasma Optical Emission Spectrometry (ICP-OES)

The ICP-OES analysis is an indirect way to determine the quantity of calcium carbonate deposited on the carbon steel sample by calcium content determination. The ICP-OES analysis is a sensitive analytical technique for determining chemical elements in several samples. It uses a high-temperature plasma to atomize and ionize samples, followed by optical emission spectrometry to identify and quantify elements in a wide range of samples. The ICP-OES analysis determined the quantity of calcium in the sample analysed, and the amount of calcium carbonate was calculated by stoichiometry.

To prepare the solutions for ICP-OES analysis, the scale layer formed in substrate was dissolved by using a Clarke's solution, prepared according to the ASTM G1-03 standard, composed of 1 L of concentrated hydrochloric acid (HCl), 20g of antimony trioxide (Sb_2O_3) and 50g stannous chloride ($SnCl_2$) (American Society for Testing and Materials, 2017). The sample with the scale deposit was immersed in 10 mL of Clarke's solution for 30 min. After this time, the solution volume was completed to 50 mL with distilled water for analysis in a Horiba ICP-OES Ultima Expert. Calcium was analysed at wavelengths 317.933 nm.

3.5.3. Scanning Electron Microscopy (SEM) coupled with energy dispersive spectroscopy (EDS)

Scanning electron microscopy was used to observe the metal surface before and after the scaling tests to verify the calcium carbonate scale formation and evaluate the crystal's morphology and distribution in the formed layer after tests. Dispersive energy spectroscopy was used to determine the chemical elements on the sample surface (semi-qualitative analysis). The SEM images, obtained using the back-scattered electron mode (accelerating voltages of 10 keV), were made using a FEI Quanta Microscope 650FEG, coupled with a Bruker EDS Quantax microanalysis system.

4. Results and discussion

4.1. Surface characterisation

Contact angle measurements were made by dripping a drop of the test solution and distilled water into the carbon steel samples roughened using abrasive papers (# 120, # 1200) and polished with 1 μm diamond paste. Fig. 4 shows the average result of triplicate tests. The results show that polished samples are more wettable (smaller contact angle), whether one uses brine or distilled water than samples roughened using #120 and #1200 abrasive papers. It is possible consider that the nucleation/substrate interface is favorable to scaling due to the contact angle being less than 180° (Cheong et al., 2013). Between the saline solution and distilled water measurements, the first one has lower contact angles. This result may be associated with the presence of electrolytes (charged ions), which can interact more with the metallic surface, resulting in a smaller contact angle.

The parameters of the roughness (R_a) of the carbon steel samples were measured in triplicate using the Taylor Hobson 3D CCI

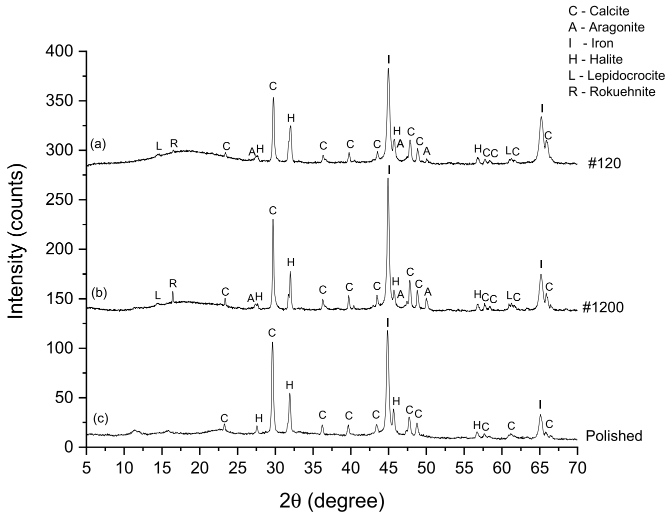

Fig. 5. XRD patterns for the 3-h scaling tests. a) Test 04: Sample roughened by abrasive paper #120. b) Test 05: Sample roughened by abrasive paper #1200. c) Test 06: polished sample (1 μm). C, A, H, I, L and R are the diffraction peaks assigned to calcite, aragonite, halite, iron, lepidocrocite and rokuehnite, respectively.

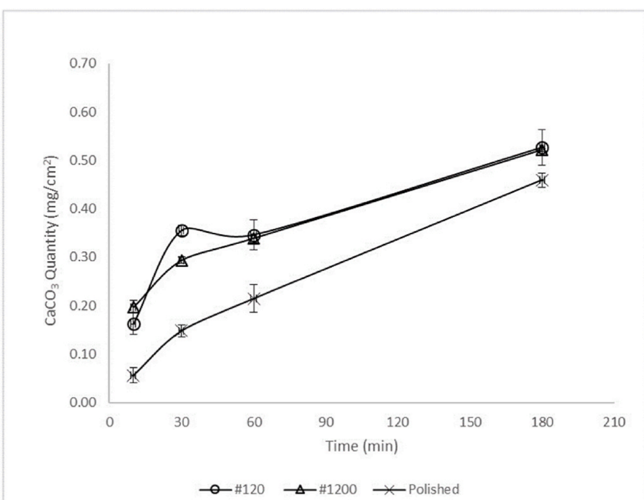

Fig. 6. Quantity of calcium carbonate in the scale layer at different roughnesses of carbon steel surfaces using ICP-OES.

profilometer. Table 2 shows the average roughness results obtained from the carbon steel samples. As expected, it can be observed that the thicker the abrasive paper used in the finishing process, the higher the surface roughness, as shown in Fig. 1.

4.2. Scaling experiments analysis

The formation of calcium carbonate scaling was observed in all performed tests indicated in Table 1. The XRD analysis was conducted for the 3-h experiments (Tests 04, 08 and 12). As can be seen in Fig. 5, for Tests 04 (# 120) and 08 (#1200), the XRD analysis detects two polymorphs calcium carbonate scale: calcite ($CaCO_3$) and aragonite ($CaCO_3$), besides halite (NaCl), iron (Fe), lepidocrocite (FeO(OH)) and rokuehnite ($FeCl_2.2H_2O$). For Test 12 (polished), the XRD analysis detects only calcite like calcium carbonate polymorph, besides halite (NaCl) and iron (Fe). Wang et al. (2013), while performing scaling experiments, observed that at a higher temperature (55 °C) the formed calcium carbonate crystals identified in the XRD analysis were calcite and aragonite. Liu et al. (2011) relate the aragonite formation with the corrosion products formation because metal ions migrate to the solution and can induce the formation of aragonite. Fig. 5 shows that lepidocrocite and rokuehnite, which are corrosion products, were not formed in the polished substrate (Test 12). This may be a possible explanation for the absence of aragonite in this test.

Additionally, Toloei et al. (2013), when studying the influence of roughness on the corrosion of nickel surfaces in diluted sulfuric acid, showed that the lower the roughness value, the more the corrosion resistance. The authors claimed that the introduction of the unidirectional roughness effectively increased the contact area between the electrolyte and the metal surface, which led to increased corrosion rates. Likewise, Abosrra et al. (2009) demonstrated that in a saline solution containing 1 and 3% NaCl, for a 316L austenitic stainless steel, the behaviour was the same: the roughest surface generated by wet grinding using SiC paper of 200-grit showed early passivity breakdown at the highest corrosion rate and lower breakdown potential compared the surfaces prepared with 600-grit or diamond polished. Conversely, another interesting result obtained in this work was for a mild steel substrate with the diamond polished surface presenting the highest corrosion rate compared with 600 and 200-grit finishing. In this way, the absence of corrosion products on the polished substrate (Fig. 5) may be attributed to a weaker confining effect of the calcium carbonate layer, which, as will be further shown in the SEM-EDS results, which did not favor the precipitation of corrosion products.

The $CaCO_3$ quantity scale which adhered to the carbon steel surface was analysed using the ICP-OES after the dissolution of the scale layer using Clarke's solution. Fig. 6 shows the results obtained from the Tests 01–04 (#120), Tests 05–08 (#1200) and Tests 09–12 (polished with 1 μm diamond paste), representing the experiments performed for 10, 30, 60 and 180 min. The data shown in Fig. 6 are the results of the difference between the average obtained in the scale tests analysis and the average obtained in the blank test. The average results of the blank test were 0.022, 0.035 and 0.037 mg of $CaCO_3/cm^2$ respectively for samples roughened by abrasive papers #120, #1200 and polished. As well as this, the bars represent the error for the test.

Observing the curves in Fig. 6, it is possible to verify that the $CaCO_3$ quantity scale increases over time for all analysed surfaces as previously

Fig. 7. Back-scattered electron SEM images for samples roughened by abrasive paper #120 (a) before scaling experiment; (b) after 10 min (Test 01); (c) after 3-h (Test 04).

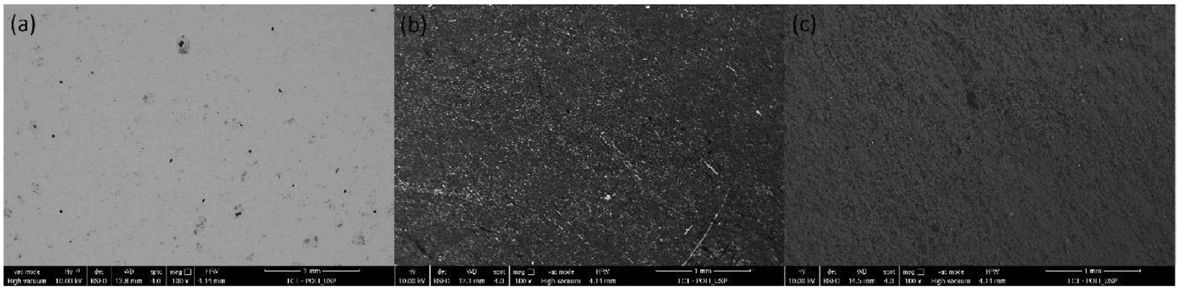

Fig. 8. Back-scattered electron SEM images for samples roughened by abrasive paper #1200 (a) before scaling experiment; (b) after 10 min (Test 05); (c) after 3-h (Test 08).

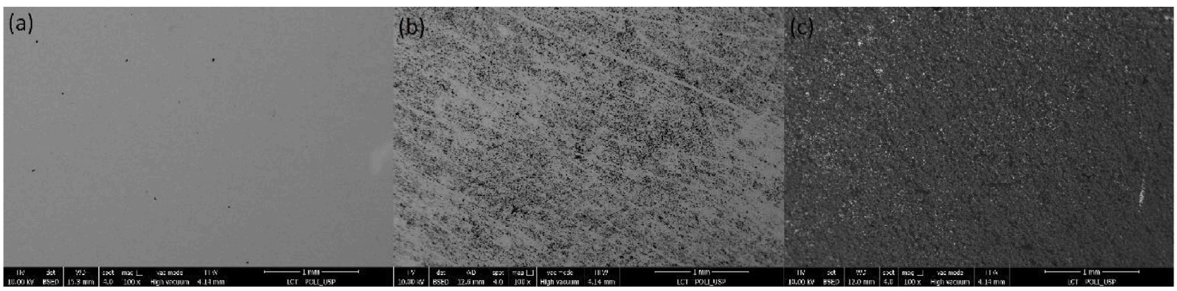

Fig. 9. Back-scattered electron SEM images for samples polished (a) before scaling experiment; (b) after 10 min (Test 09); (c) after 3-h (Test 12).

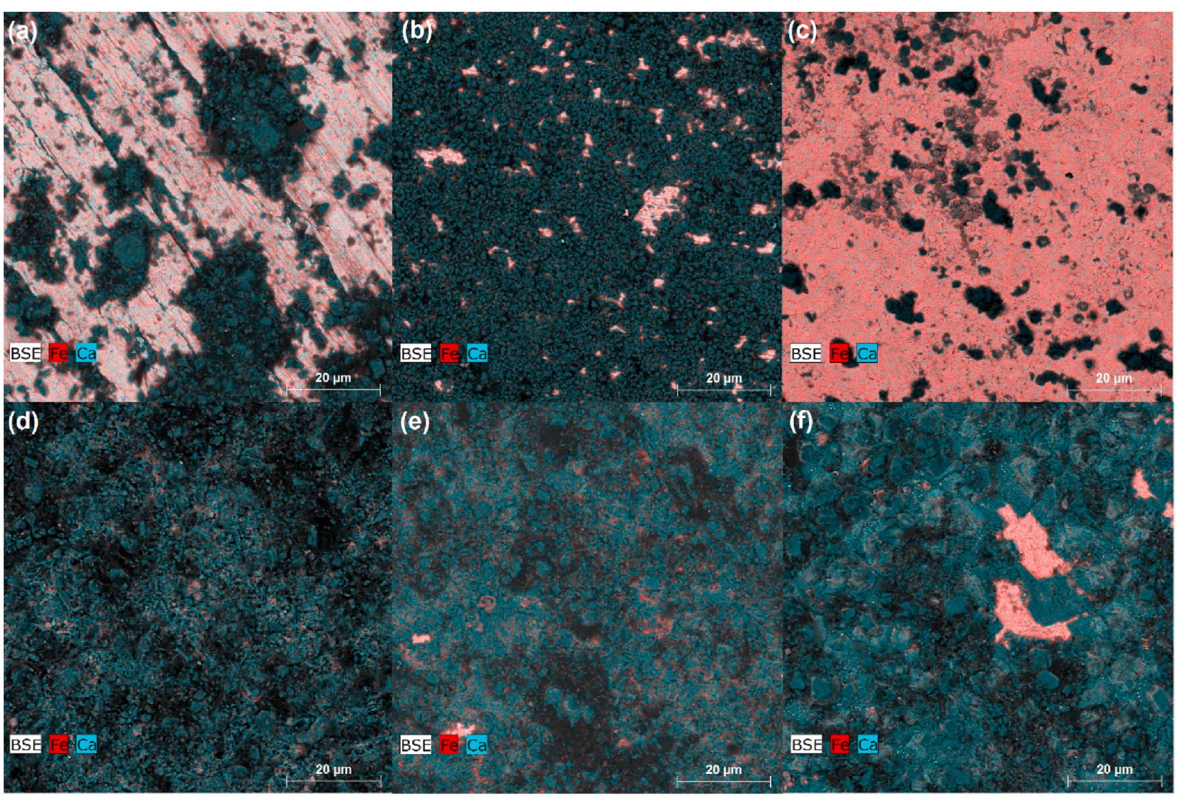

Fig. 10. EDS mapping analysis. (a) Test 01 (#120 - 10 min); (b) Test 05 (#1200 - 10 min); (c) Test 09 (polished - 10 min); (d) Test 04 (#120 - 3 h); (e) Test 08 (#1200 - 3 h); (f) Test 12 (polished - 3 h).

noted by Cheong et al. (2013).

Comparing results obtained in the ICP analysis for the different samples in Fig. 6, the difference between the quantity of $CaCO_3$ adhered to the carbon steel for samples roughened by abrasive paper #120 and #1200 is not significant. However, the quantity of $CaCO_3$ in the scale adhered to the polished surface was smaller compared to the others, which may indicate that substrates with a much lower roughness (smoother surface), are less prone to calcium carbonate scaling, as already observed in other studies such as Alahmad (2008), Eroini et al. (2011) and Keysar et al. (1994).

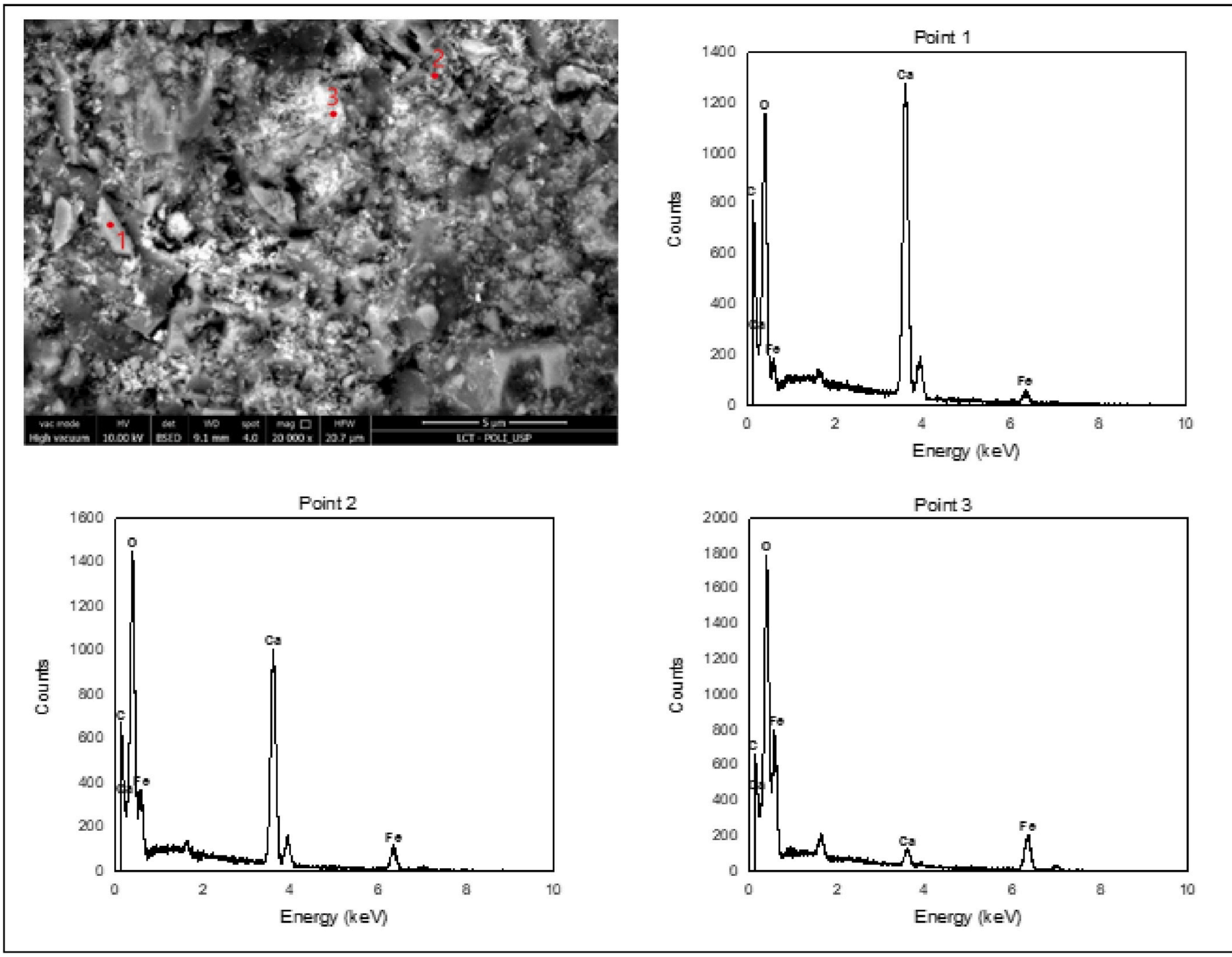

Fig. 11. Back-scattered electron SEM images with semi-qualitative analysis using dispersive energy spectroscopy (EDS) of the selected regions of the Test 04 (#120 - 3-h).

The SEM images shown in Figs. 7–9 correspond to samples before scaling experiments, after 10-min (Tests 01, 05 and 09) and after 3-h (Tests 04, 08 and 12). Initially, comparing the SEM images of before (Figs 7a, 8a and 9a) and after scaling experiments (Figs. 7b–c, 8b–c and 9b–c), it can be observed that there is a layer adhered to the surface, indicating the scale formation. However, it is possible to observe that in the 3-h experiments (Figs. 7c, 8c and 9c) the scale layer formed is thicker than in the 10-min experiments (Figs. 7b, 8b and 9b), showing that the formation of calcium carbonate scale has already been formed since the beginning of the experiment run, increasing the deposit formed over time. It is also possible to observe grooves in the images of the 10-min experiments (Figs. 7b, 8b and 9b), indicating that the scale layer formed in this period is not tough, as a deposited material quantity is detached from the substrate by of the flow, which is not possible to observe in the 3-h experiment images (Figs. 7c, 8c and 9c).

The EDS mapping analysis shows the distribution of the elements deposited on the sample surface after the experiments were carried out. Fig. 10 shows the analysis results in terms of iron and calcium elements. The iron element can be present in the substrate and is represented by the red colour, and the calcium element can be present in the calcium carbonate scale and is represented by the blue colour. Fig. 10a–c shows images of 10 min of tests (Tests 01, 05 and 09) and Fig. 10d–f shows 3-h of tests (Tests 04, 08 and 12). As previously noted, the images taken after 10 min of tests show a smaller amount of scale, with part of the substrate exposed (red colour), in contrast to what occurs in the 3-h tests, where the presence of calcium predominates (blue colour). By comparing the 10 min tests images, it is possible to observe that the sample roughened by abrasive paper #120 has larger crystals in relation to the other two samples and that the polished sample had fewer crystals than the others. Comparing the 3-h test images, it is also possible to observe that the polished sample had fewer crystals in relation to the other two and that the sample roughened using abrasive paper #1200 had fewer crystals than the sample roughened by abrasive paper #120.

Figs. 11 and 12 are examples of results from the EDS microanalysis for the 3-h experiments carried out with the samples roughened by abrasive paper #120 (Test 04) and polished with 1 μm diamond paste (Test 12), respectively. It can be observed that, in general, in these deposits, carbon (C), oxygen (O) and calcium (Ca) elements are present, which can be associated with calcium carbonate. The conclusion regarding the presence of calcium carbonate crystals by SEM/EDS analysis was based on the results of X-ray diffraction, which confirmed the presence of this salt (Fig. 5).

Point 3 of Fig. 12 (Test 12 - polished – 3-h) can represent a failure in the scale coverage, due to the high content of iron present (carbon steel substrate). This observation can indicate that there is less scale formation or less scale adhesion on this type of surface. The other points that have iron (Fe) associated with the other elements can represent the presence of corrosion products, as seen previously in the analysis of X-

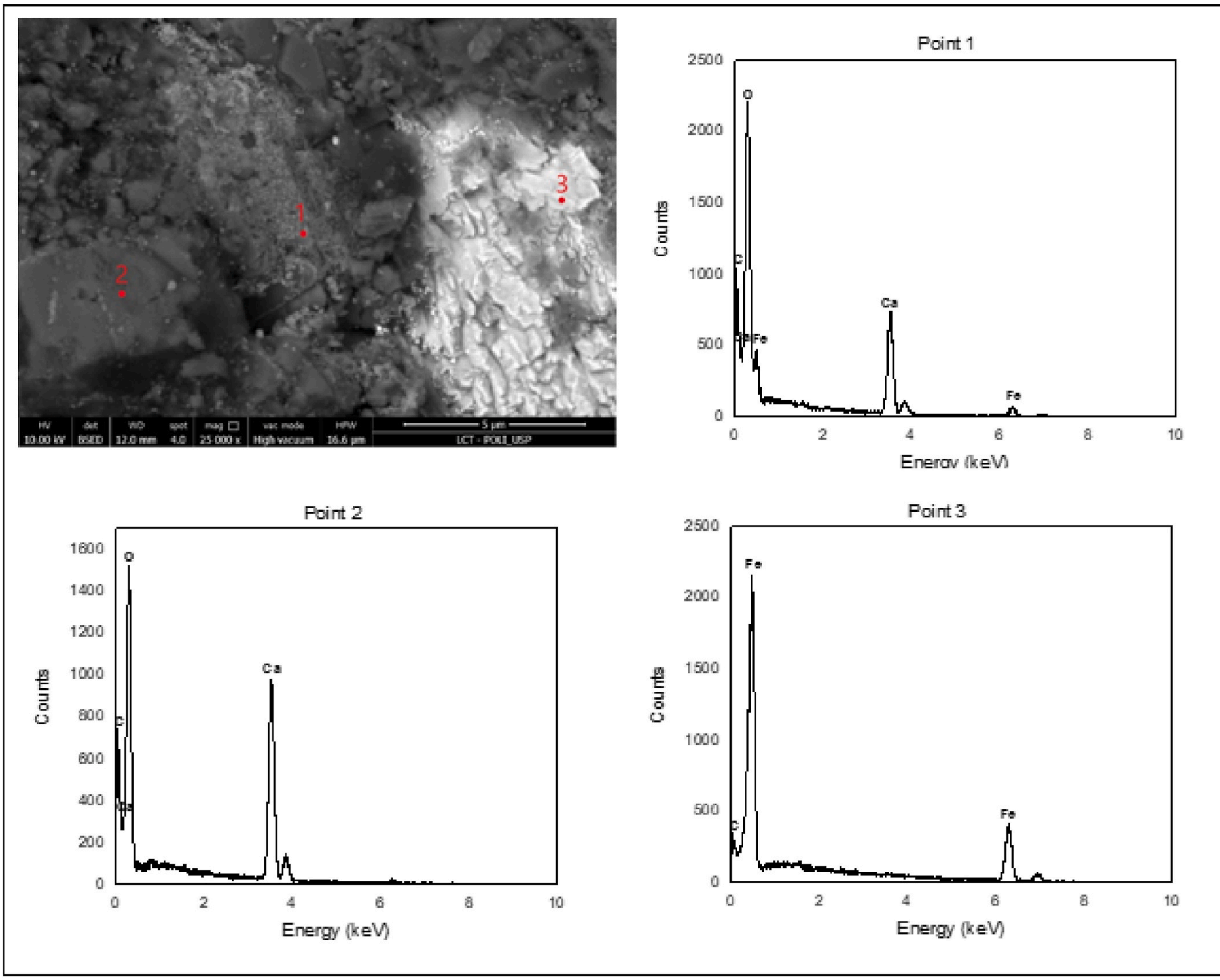

Fig. 12. Back-scattered electron SEM images with semi-qualitative analysis by dispersive energy spectroscopy (EDS) of the selected regions of the Test 12 (polished - 3-h).

ray diffraction.

The Electron scattered SEM images with magnification 30000x, represented by Fig. 13a–f, show that the crystals are deposited and/or formed randomly on the surfaces, without orientation. Regarding the deposits formed, it is possible to observe cubic and stick morphology crystals and more amorphous crystals. Some of these morphologies were found by Eroini et al. (2011), Liu et al. (2011) and Wang et al. (2013). In these studies, it is mentioned that the calcium carbonate morphology, associated with calcite, has a cubic shape and aragonite has a stick shape, in addition to their amorphous forms. Aragonite (stick morphology) was found in the Test 04 and 08 (3-h experiments with samples roughened with abrasive papers #120 and #1200, respectively) (Fig. 13d–e). In the Test 12 (polished -3-h experiment) (Fig. 13f) it seems to have few or no presence of this form of calcium carbonate. These results had previously been observed using X-ray diffraction analysis (Fig. 5). Aragonite is formed when corrosion products are also formed (Liu et al., 2011) and lepidocrocite and rokuehnite, which are corrosion products, were detected only in the samples roughened with abrasive papers #120 (Test 04) and #1200 (Test 08), on the polished substrate (Test 12) was not detected.

Analysing the 10 min experiments images (Tests 01, 05 and 09) (Fig. 13a–c) it is possible to observe that 10 min is enough for the calcium carbonate scale to form on the substrate on all tested surfaces. Comparing the 10 min experiment images (Fig. 13a–c) with the 3-h experiment images (Fig. 13d–f), it is possible to observe that the size and quantity of crystals are higher for the 3-h experiments, indicating that the quantity of calcium carbonate scale and crystal size increases over time.

Comparing the image of the Test 04 (#120 - 3-h) (Fig. 13d) with the images from the Test 08 (#1200 - 3-h) (Fig. 13e) and Test 12 (polished – 3-h) (Fig. 13f), it is possible to verify that, in general, the quantity and size of crystals formed on the surfaces roughened by #120 abrasive paper are larger than those formed on surfaces roughened by #1200 abrasive paper and polished. The same comparison can be made only between the images of the experiments in which the samples were roughened using #1200 abrasive paper (Test 08) (Fig. 13e) and polished (Test 12) (Fig. 13f), proving that, in general, the quantity and size of crystals formed on the surfaces roughened by #1200 abrasive paper is larger than those formed on polished surfaces. With these observations, it is possible to deduce that samples roughened using #120 abrasive paper, may be more susceptible to scale formation, followed by samples roughened by #1200 abrasive paper and polished.

5. Conclusions

Scaling tests were conducted using a set-up composed of a peristaltic

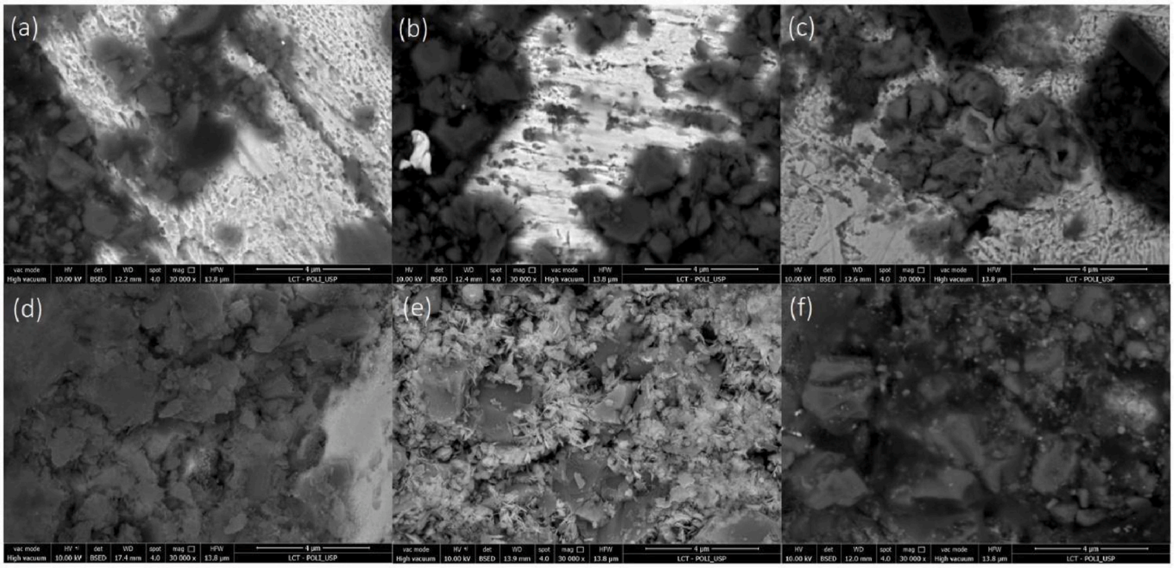

Fig. 13. Back-scattered electron SEM images (30000x magnification). (a) Test 01 (#120 - 10 min); (b) Test 05 (#1200 - 10 min); (c) Test 09 (polished - 10 min); (d) Test 04 (#120 - 3-h); (e) Test 08 (#1200 - 3-h); (f) Test 12 (polished - 3-h).

pump to recirculate the test solution through a flow cell. The formation of the calcium carbonate was obtained using a brine containing a calcium content close to that found in the pre-salt produced water on a carbon steel surface with different levels of roughness. The scale build-up that adhered to the surface was analysed chemically and microstructurally. The following findings were obtained.

In all scaling experiments, the formation of calcium carbonate scale was observed. Experiments carried out over shorter periods formed less tenacious layers, whereas experiments carried out over longer periods formed a more adherent layer of scale.

The quantity of calcium carbonate scale adhered to the substrate surface, and the size of calcium carbonate crystals increases over time on all analysed surfaces (Sanni et al., 2017).

The calcium carbonate polymorphs formed was predominantly calcite. Lepidocrocite and rokuehnite, which are corrosion products, were formed in the substrates with higher roughness values (# 120 and #1200), promoting aragonite formation (Liu et al., 2011).

The rougher the steel sample, the greater the quantity of calcium carbonate scale adhered to the substrate, resulting in the conclusion that for steel substrates, greater roughness may be more susceptible to calcium carbonate scale formation (Alahmad, 2008; Cheong et al., 2013; Eroini et al., 2011; Keysar et al., 1994).

For steel substrate, surface roughness influenced the scaling and corrosion processes besides affecting the calcium carbonate polymorphs (Liu et al., 2011).

Credit author statement

Juliana Francisco de Angelo: Conceptualization, Methodology, Writing – original draft preparation, Validation, Investigation, Visualization Jean Vicente Ferrari: Conceptualization, Methodology, Writing – review & editing, Supervision, Resources.

Funding

This work was partially supported by the Coordenação de Aperfeiçoamento de Pessoal de Nível Superior (CAPES/Brazil) - Ph.D. Grant

Declaration of competing interest

The authors declare that they have no known competing financial interests or personal relationships that could have appeared to influence the work reported in this paper.

Data availability

The authors do not have permission to share data.

Acknowledgments

We want to thank the following laboratories and research groups at the Polytechnic School of the Universidade de São Paulo (Poli-USP) for their support in the analysis: Laboratório de Caracterização Tecnológica (LCT), Laboratório de Fenômenos de Transporte e Físico-Química de Interfaces (LFQI) and the Integrated Technologies for Rock and Fluid Analysis (InTRA) group.

References

Abosrra, L., Ashour, A.F., Mitchell, S.C., Youseffi, M., 2009. Corrosion of mild steel and 316L austenitic stainless steel with different surface roughness in sodium chloride saline solutions. WIT Trans. Eng. Sci. 65, 161–172. https://doi.org/10.2495/ECOR090161.

Alahmad, M., 2008. Factors affecting scale formation in sea water environments - an experimental approach. Chem. Eng. Technol. 31, 149–156. https://doi.org/10.1002/ceat.200700062.

American Society for Testing and Materials, 2017. In: ASTM G1-03: Standard Practice for Preparing, Cleaning, and Evaluating Corrosion Test Specimens. https://doi.org/10.1520/G0001-03R11.2.

Beltrao, R.L., Sombra, C.L., Lage, A.C.V.M., Fagundes Netto, J.R., Henriques, C.C.D., Petrobras, 2009. Challenges and new technologies for the development of the pre-salt cluster, Santos Basin, Brazil. In: Offshore Technology Conference, 2009, Houston. Offshore Technology Conference, pp. 1–11. https://doi.org/10.4043/19880-MS. Houston.

Bezerra, M.C.M., Rosário, F.F., Rosa, K.R.S. a, 2013. Scale management in deep and ultradeep water fields. In: Offshore Technology Conference Brasil, 2013, Rio de Janeiro. Offshore Technology Conference, pp. 1–13. Rio de Janeiro.

Cezar, A.S.P., Pereira, A.R., Daniel, L.L., Oazen, E.V., Trovoado, L.C., De Almeida, M.C., 2015. Subsea solutions in the pre-salt development projects. In: Offshore Technology Conference, 2015, Houston. Offshore Technology Conference, pp. 1–20. https://doi.org/10.4043/25773-MS. Houston.

Chaussemier, M., Pourmohtasham, E., Gelus, D., Pécoul, N., Perrot, H., Lédion, J., Cheap-Charpentier, H., Horner, O., 2015. State of art of natural inhibitors of calcium carbonate scaling. A review article. Desalination 356, 47–55. https://doi.org/10.1016/j.desal.2014.10.014.

Chen, T., Neville, A., Yuan, M., 2005. Calcium carbonate scale formation - assessing the initial stages of precipitation and deposition. J. Pet. Sci. Eng. 46, 185–194. https://doi.org/10.1016/j.petrol.2004.12.004.

Cheong, W.C., Gaskell, P.H., Neville, A., 2013. Substrate effect on surface adhesion/crystallisation of calcium carbonate. J. Cryst. Growth 363, 7–21. https://doi.org/10.1016/j.jcrysgro.2012.09.025.

Crabtree, M., Eslinger, D., Fletcher, P., Miller, M., Johnson, A., King, G., 1999. Fighting scale — removal and prevention. Oilfield Rev. 11, 30–45.

Drexler, S., Correia, E.L., Jerdy, A.C., Cavadas, L.A., Couto, P., 2020. Effect of CO2 on the dynamic and equilibrium interfacial tension between crude oil and formation brine for a deepwater Pre-salt field. J. Pet. Sci. Eng. 190, 107095 https://doi.org/10.1016/j.petrol.2020.107095.

Droguett, E.L., Lins, I.D., Moura, M.C., Zio, E., Jacinto, C.M., 2015. Variable selection and uncertainty analysis of scale growth rate under pre-salt oil wells conditions using support vector regression. J. Risk Reliab. 229, 319–326. https://doi.org/10.1177/1748006X14533105.

Eroini, V., Kapur, N., Neville, A., Euvrard, M., 2011. Preventing scale formation using modified surfaces. In: Corrosion, 2011, Houston. NACE International, Houston, pp. 1–15.

Hashimoto, R., Morita, M., Umezawa, O., Motoda, S., 2017. Effect of ions eluted from metal surface on transformation and growth of calcium carbon- ate polymorphisms. J. Japan Inst. Meals Mater. 81, 89–96. https://doi.org/10.2320/jinstmet.J2016045.

Hidema, R., Toyoda, T., Suzuki, H., Komoda, Y., Shibata, Y., 2016. Adhesive behavior of a calcium carbonate particle to solid walls having different hydrophilic characteristics. Int. J. Heat Mass Tran. 92, 603–609. https://doi.org/10.1016/j.ijheatmasstransfer.2015.08.068.

Kamal, M.S., Hussein, I., Mahmoud, M., Sultan, A.S., Saad, M.A.S., 2018. Oilfield scale formation and chemical removal: a review. J. Pet. Sci. Eng. 171, 127–139. https://doi.org/10.1016/j.petrol.2018.07.037.

Kelland, M.A., 2009. Production Chemicals for the Oil and Gas Industry, first ed. CRC Press Taylor & Francis Group, Boca Raton.

Keysar, S., Semiat, R., Hasson, D., Yahalom, J., 1994. Effect of surface roughness on the morphology of calcite crystallizing on mild steel. J. Colloid Interface Sci. 162, 311–319. https://doi.org/10.1006/jcis.1994.1044.

Liu, Y., Zou, Y., Zhao, L., Liu, W., Cheng, L., 2011. Investigation of adhesion of CaCO3 crystalline fouling on stainless steel surfaces with different roughness. Int. Commun. Heat Mass Tran. 38, 730–733. https://doi.org/10.1016/j.icheatmasstransfer.2011.04.003.

Liu, Y., Kan, A.T., Tomson, M.B., Zhang, P., 2022. Interactions of common scale inhibitors and formation mineral (calcium carbonate): sorption and transportability investigations under equilibrium and dynamic conditions. J. Pet. Sci. Eng. 215, 110696 https://doi.org/10.1016/j.petrol.2022.110696.

Maciel, R.S., Cosmo, R.P., Maciel, F.S., Pereira, F.A.R., Ribeiro, D.C., Federal, U., 2017. On the hydrodynamic aspects of the carbonate scale formation process in high flow rate wells. In: Offshore Technology Conference Brasil, 2017, Rio De Janeiro. Offshore Technology Conference, pp. 1–15. Rio de Janeiro.

Marques, L.C.C., Pereira Jr., a Z.I., R.O.M, Gonçalves, M. a C., 2001. How petrobras has faced oilfield scale problems : evolution of concepts and lessons learned in campos basin, Brazil. In: SPE International Symposium on Oilfield Scale, 2001. Aberdeen. Society of Petroleum Engineers, Aberdeen, pp. 1–4. https://doi.org/10.2523/68327-MS.

Neville, A., Morizot, A.P., 2000. A combined bulk chemistry/electrochemical approach to study the precipitation, deposition and inhibition of CaCO3. Chem. Eng. Sci. 55, 4737–4743. https://doi.org/10.1016/S0009-2509(00)00046-4.

Olajire, A.A., 2015. Journal of Petroleum Science and Engineering A review of oil fi eld scale management technology for oil and gas production. J. Pet. Sci. Eng. 135, 723–737. https://doi.org/10.1016/j.petrol.2015.09.011.

Palmer, A.C., King, R.A., 2004. Subsea Pipeline Engineering, first ed. PennWell Books, Tulsa.

Pomini, A.M., 2013. A Química na Produção de Petróleo, first ed. Editora Interciência, Rio de Janeiro.

Qazvini, S., Golkari, A., Azdarpour, A., Santos, R.M., Safavi, M.S., Norouzpour, M., 2021. Experimental and modelling approach to investigate the mechanisms of formation damage due to calcium carbonate precipitation in carbonate reservoirs. J. Pet. Sci. Eng. 205, 108801 https://doi.org/10.1016/j.petrol.2021.108801.

Sanni, O., Bukuaghangin, O., Huggan, M., Kapur, N., Charpentier, T., Neville, A., 2017. Development of a novel once-Through flow visualization technique for kinetic study of bulk and surface scaling. Rev. Sci. Instrum. 88, 103903 https://doi.org/10.1063/1.4991729.

Santana, C.J., Manzela, A.A., 2016. Incrustações inorgânicas em campos do pré-sal. Rev. Eng. da Fac. Sales. 4, 22–31.

Telles, P.C.S., 2001. Tubulações Industriais - Materiais, Projeto, Montagem, tenth ed. LTC, Rio de Janeiro.

Toloei, A., Stoilov, V., Northwood, D., 2013. The relationship between surface roughness and corrosion. In: ASME 2013 International Mechanical Engineering Congress and Exposition, vol. 2B. ASME, San Diego. https://doi.org/10.1115/IMECE2013-65498. Advanced Manufacturing.

Vazirian, M.M., Charpentier, T.V.J., de Oliveira Penna, M., Neville, A., 2016. Surface inorganic scale formation in oil and gas industry: as adhesion and deposition processes. J. Pet. Sci. Eng. 137, 22–32. https://doi.org/10.1016/j.petrol.2015.11.005.

Wang, Z., Neville, A., Meredith, A.W., 2005. How and why does scale stick— can the surface Be engineered to decrease scale formation and adhesion?. In: SPE International Symposium on Oilfield Scale, 2005. Aberdeen. Society of Petroleum Engineers, Aberdeen, pp. 1–8. https://doi.org/10.2118/94993-MS.

Wang, H., Alfredsson, V., Tropsch, J., Ettl, R., Nylander, T., 2013. Formation of CaCO3 deposits on hard surfaces - effect of bulk solution conditions and surface properties. ACS Appl. Mater. Interfaces 5, 4035–4045. https://doi.org/10.1021/am401348v.

Wang, L.-C., Li, S.-F., Wang, L-Bi, Cui, K., Zhang, Q.-L., Liu, H.-B., Li, G., 2016. Relationships between the characteristics of CaCO3 fouling and the flow velocity in smooth tube. Exp. Therm. Fluid Sci. 74, 143–159. https://doi.org/10.1016/j.expthermflusci.2015.12.001.

Yamanaka, S., Ito, N., Shimosaka, A., Shirakawa, Y., Hidaka, J., 2009. AFM investigation for the initial growth processes of calcium carbonate on hydrophilic and hydrophobic substrate. Cryst. Growth Des. 9, 3245–3250. https://doi.org/10.1021/cg801334g.

Zettler, H.U., Weiß, M., Zhao, Q., Müller-Steinhagen, H., 2005. Influence of surface properties and characteristics on fouling in plate heat exchangers. Heat Tran. Eng. 26, 3–17. https://doi.org/10.1080/01457630590897024.